

Photodissociation spectroscopy of protonated leucine enkephalin

Andreas Herburger, Christian van der Linde and Martin K. Beyer*

*Institut für Ionenphysik und Angewandte Physik, Leopold-Franzens-Universität Innsbruck,
Technikerstraße 25, 6020 Innsbruck, Austria*

Electronic Supplementary Information

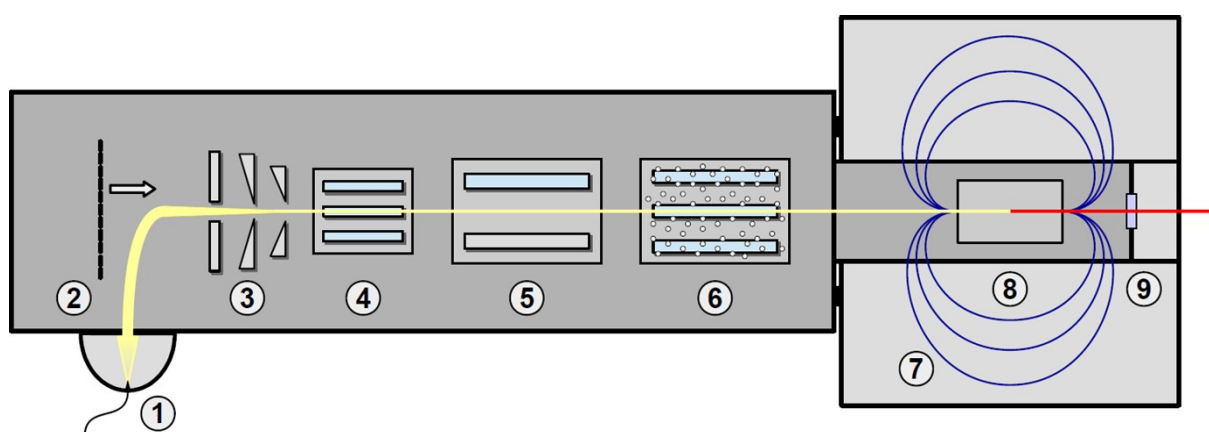


Figure S1. Simplified schematic view of the commercial FT-ICR MS Bruker APEX Qe: **1)** Electro spray Source, **2)** Repeller, **3)** Electrostatic Lens and two Funnel, **4)** Hexapole, **5)** Quadrupole Mass Filter, **6)** Collision Cell, **7)** 9.4 T Superconducting Magnet, **8)** ICR Cell, **9)** Window for Laser Irradiation. Note that the cyclotron radius is smaller than the diameter of the laser beam. Additional electrostatic lenses for ion guiding are placed in between **4)**, **5)**, **6)** and **8)**.

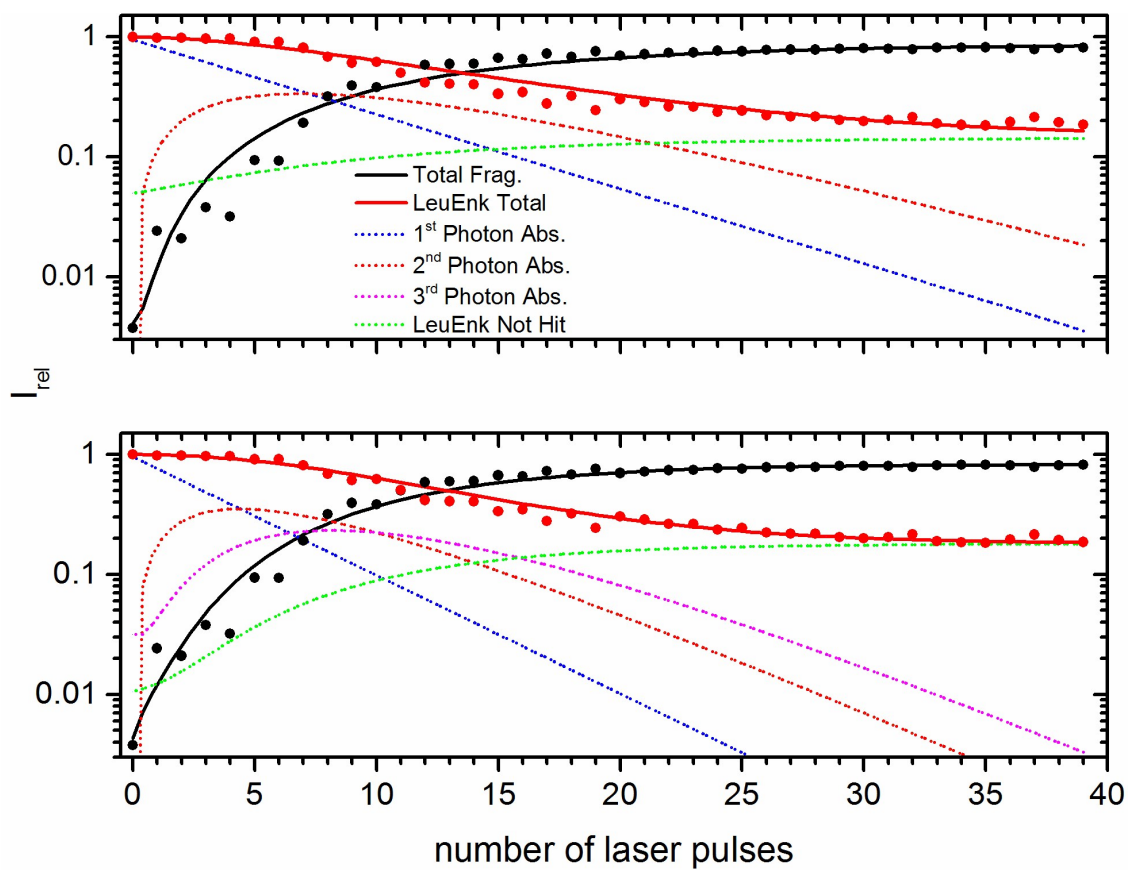


Figure S2: Kinetics fit assuming sequential absorption of two (top) and three photons (bottom).

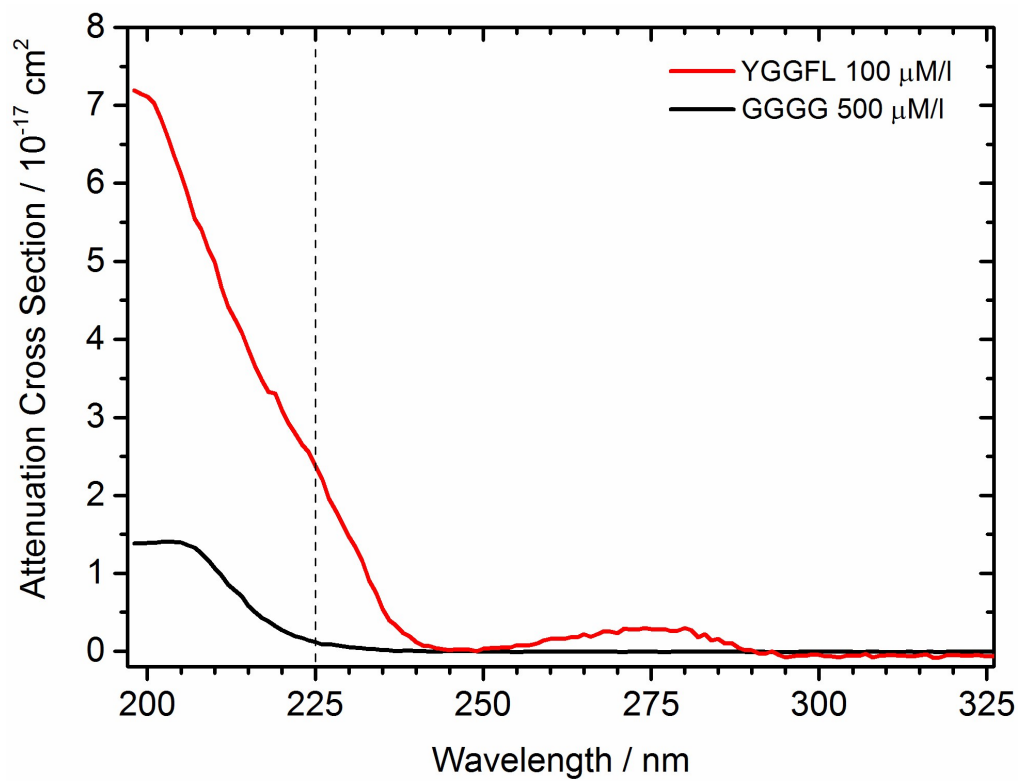


Figure S3: Solution phase UV-VIS spectrum of YGGFL and GGGG for comparison.

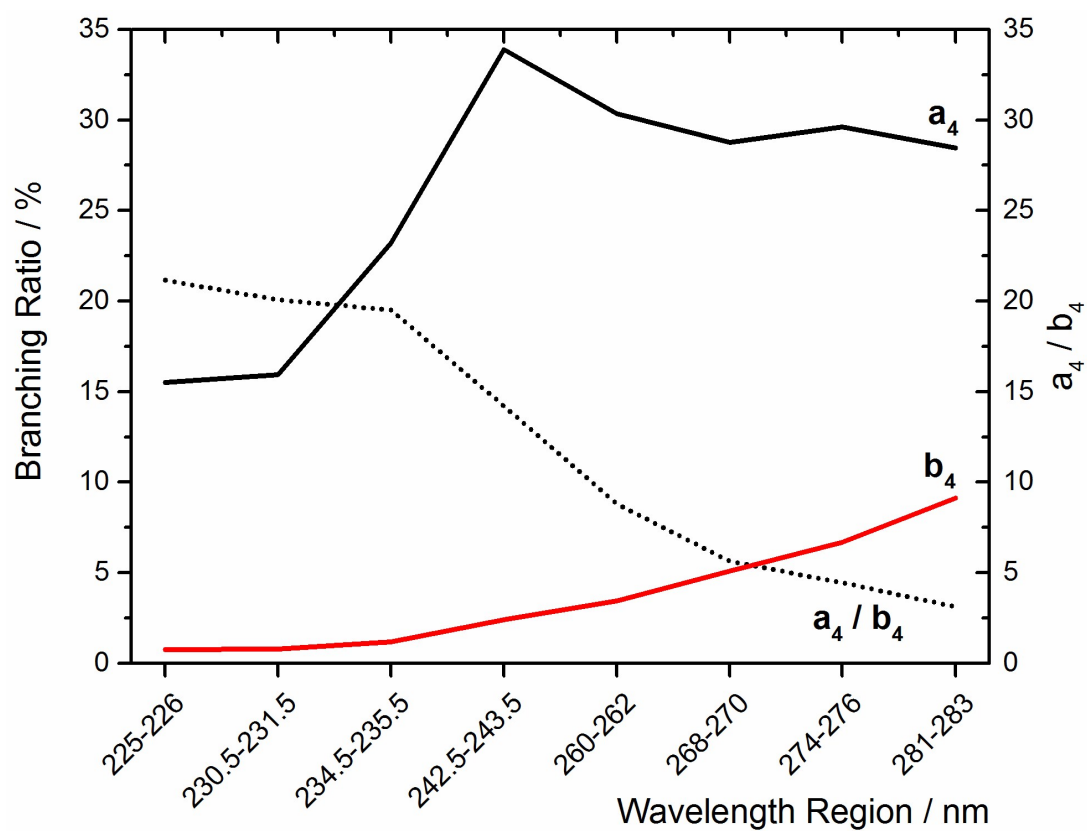


Figure S4: Ratio of a_4 vs. b_4 as a function of wavelength.

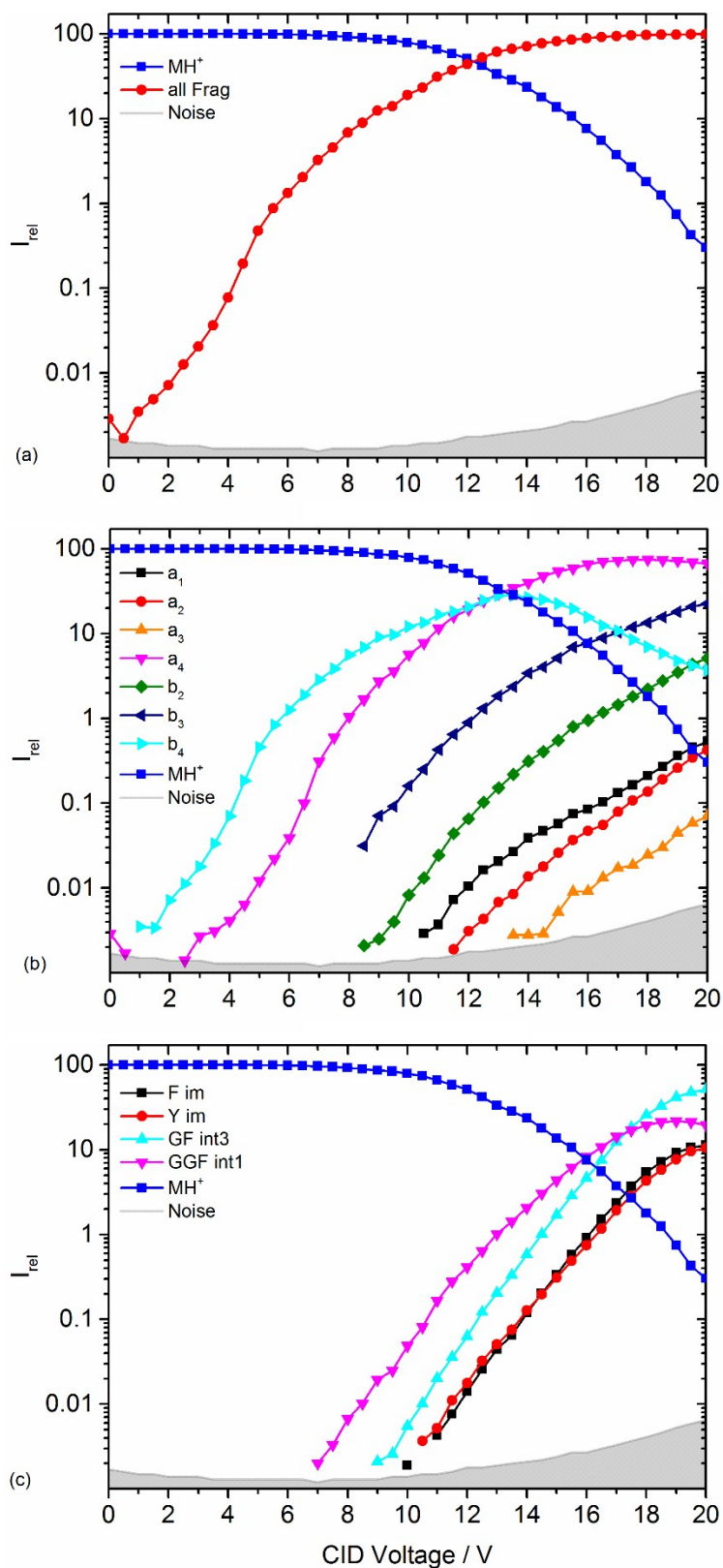


Figure S5: (a) Collision induced dissociation of protonated leucine enkephalin with argon for CID voltages from 0 to 20 V (< 1% of precursor ion remaining). (b) a- and b-type fragments and (c) internal fragments. All abundant ions have been included into the analysis.

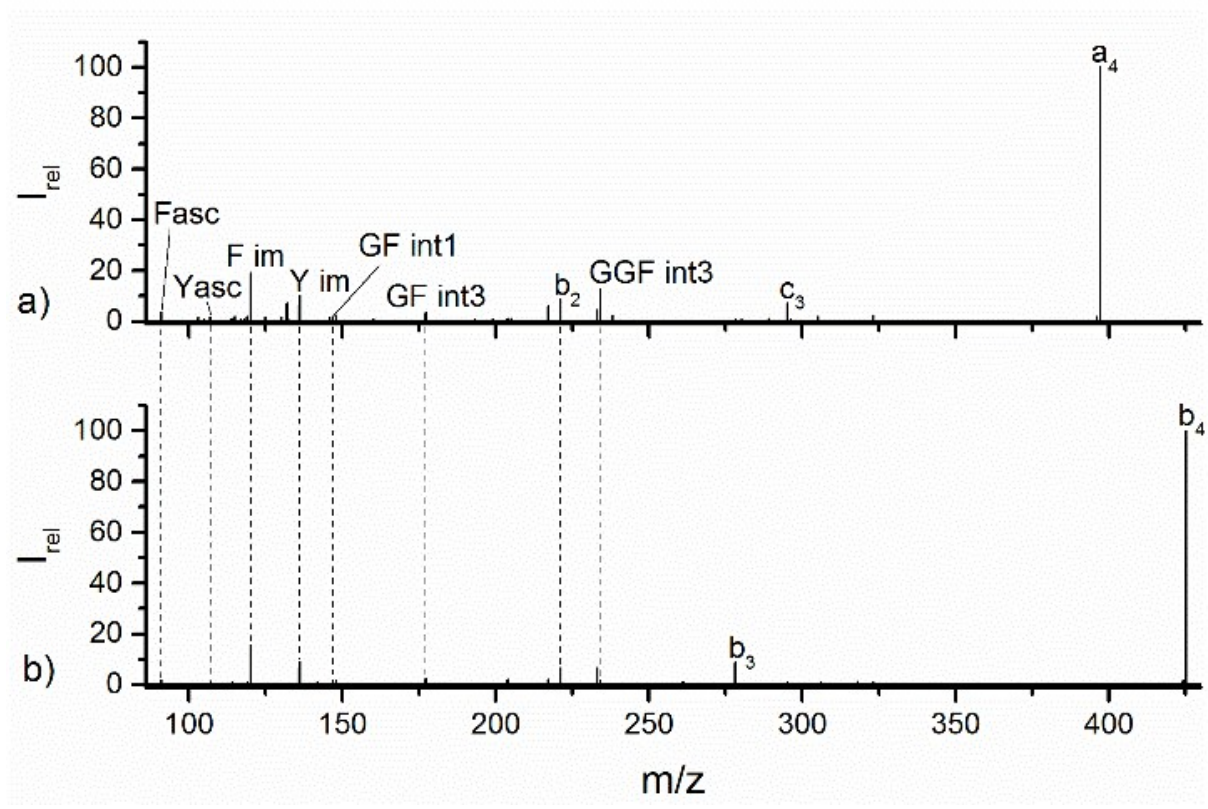


Figure S6: Fragment-LID: Mass spectra after irradiation of a_4 (a) and b_4 (b) for 1 sec. Mainly small (higher order) side chain and internal fragments are formed.

Table S1. List of all identified singly protonated sequence fragments upon LID (incl. protonated YGGFL). Measured mass, expected exact mass and deviation between measured and exact mass.

Fragment	$m_{\text{meas}} / \text{Da}$	$m_{\text{exact}} / \text{Da}$	$\Delta m / \text{mDa}$
a ₁	136.0764	136.0762	0.1
a ₂	193.0980	193.0977	0.3
a ₃	250.1195	250.1192	0.4
a ₄	397.1874	397.1876	0.2
b ₁	164.0714	164.0712	0.2
b ₂	221.0930	221.0926	0.3
b ₃	278.1144	278.1141	0.3
b ₄	425.1823	425.1825	0.3
c ₁	181.0980	181.0977	0.3
c ₂	238.1198	238.1192	0.6
c ₃	295.1449	295.1407	4.3
x ₃	362.1715	362.1716	0.1
x ₄	419.1928	419.1931	0.3
y ₁	132.1026	132.1025	0.1
y ₂	279.1711	279.1709	0.2
y ₃	336.1925	336.1924	0.1
y ₄	393.2137	393.2138	0.1
(YGGFL)H ⁺	556.2761	556.2772	1

Table S2. List of re-assignments for LID.

Previous assignment	Reassignment	$m_{\text{meas}} / \text{Da}$	$m_{\text{exact}} / \text{Da}$	$\Delta m / \text{mDa}$
z ₁	GGF int4+H	115.0508	115.0508	0.07
x ₁	YGGF int3+H	158.0608	158.0566	4.2
z ₂	YGGF int1	262.1194	262.1192	0.2
x ₂	YGGFL int1	305.1252	305.1250	0.2

Table S3. List of all identified singly protonated internal and side chain fragments upon LID, as well as two intense unassigned fragment peaks iu1 and iu2. Measured mass, expected exact mass and deviation between measured and exact mass.

Fragment	$m_{\text{meas}} / \text{Da}$	$m_{\text{exact}} / \text{Da}$	$\Delta m / \text{mDa}$
F asc	91.0547	91.0548	0.05
Y asc	107.0497	107.0497	0.03
GGF int4+H	115.0508	115.0508	0.07
F im	120.0814	120.0813	0.04
Y im	136.0764	136.0762	0.1
GFint1	147.0686	147.0684	0.2
YGGF int3+H	158.0608	158.0566	4.2
GF int2	162.0921	162.0919	0.2
GF int3	177.1030	177.1028	0.2
GGF int1	205.0979	205.0977	0.2
GGF int2	219.1137	219.1134	0.4
GGF int3	234.1246	234.1243	0.3
YGGF int1	262.1194	262.1192	0.2
YGGF int2	290.1143	290.1141	0.2
YGGFL int1	305.1252	305.1250	0.2
iu1	323.1403		
y ₄ ^o	375.2033	375.2033	0.05
a ₄ [*]	380.1610	380.1611	0.01
Iu2	426.1675		
MH ⁺ -Y asc-H	448.2207	448.2196	1.1
MH ⁺ -Y asc	449.2271	449.2275	0.3
MH ⁺ -F asc	465.2220	465.2224	0.4
MH ⁺ -(NH ₃ ⁺ +HCOOH)	493.2444	493.2451	0.7
MH ⁺ -HCOOH	510.2708	510.2717	0.8
MH ⁺ -H ₂ O	538.2654	538.2666	1

Table S4. Center position of Gaussian fit functions in Figure 4.

1-Photon / cm^{-1}	2-Photon / cm^{-1}	3-Photon / cm^{-1}	Average
52000	52000	52000	
38375	38420	38271	38355
36730	36646	36713	36696
35481	35448	35428	35452
		34053	

Table S5. List of all identified singly protonated fragments upon CID (incl. protonated YGGFL). Measured mass, expected exact mass and deviation between measured and exact mass.

Fragment	$m_{\text{meas}} / \text{Da}$	$m_{\text{exact}} / \text{Da}$	$\Delta m / \text{mDa}$
a ₁	136.0761	136.0762	0.1
a ₂	193.0977	193.0977	0.04
a ₃	250.1192	250.1192	0.006
a ₄	397.1875	397.1876	0.1
b ₂	221.0927	221.0926	0.02
b ₃	278.1142	278.1141	0.1
b ₄	425.1818	425.1825	0.7
c ₁	181.0977	181.0977	0.02
c ₂	238.1232	238.1192	4
c ₃	295.1447	295.1407	4
x ₄	419.1920	419.1931	1
y ₁	132.1023	132.1025	0.2
y ₂	279.1710	279.1709	0.1
y ₃	336.1925	336.1924	0.1
y ₄	393.2134	393.2138	0.5
F im	120.0812	120.0813	0.2
Y im	136.0761	136.0762	0.1
GF int3	177.1027	177.1028	0.07
GGF int1	205.0977	205.0977	0.03
y ^o ₄	375.2034	375.2033	0.2
a [*] ₄	380.1613	380.1612	0.2
MH ⁺ -SC	465.2503	465.2502	0.1
MH ⁺ -(NH ₃ +HCOOH)	493.2458	493.2451	0.6
MH ⁺ -HCOOH	510.2725	510.2717	0.8
MH ⁺ -H ₂ O	538.2670	538.2666	0.4
(YGGFL)H ⁺	556.2779	556.2772	0.7

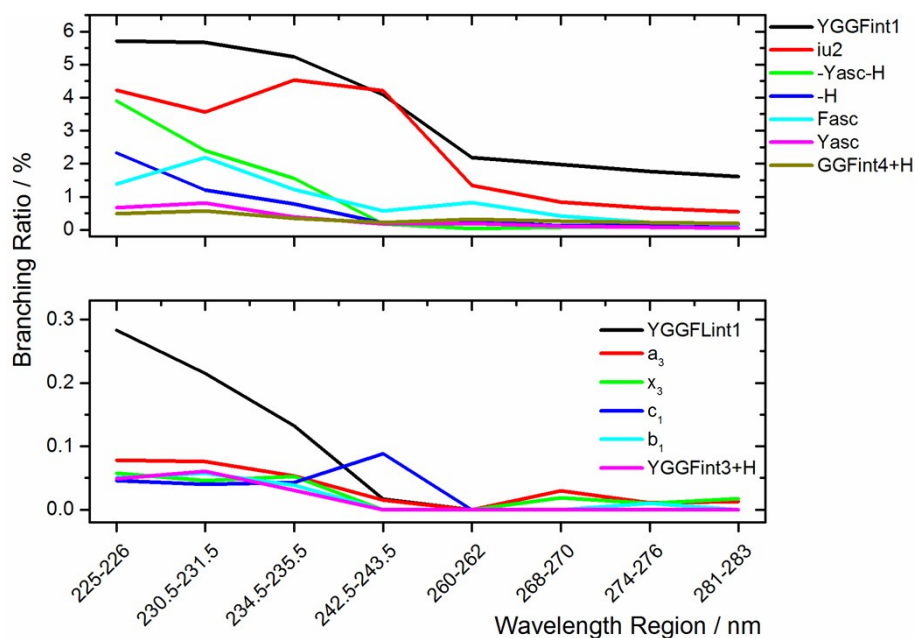
Table S6. List of re-assignments for previously published CID fragments.

Previous assignment	Re-assignment	$m_{\text{meas}} / \text{Da}$	$m_{\text{exact}} / \text{Da}$	$\Delta m / \text{mDa}$
MH ⁺ -F asc	MH ⁺ -SC	465.2503	465.2502	0.1

Wavelength dependence of fragment branching ratios

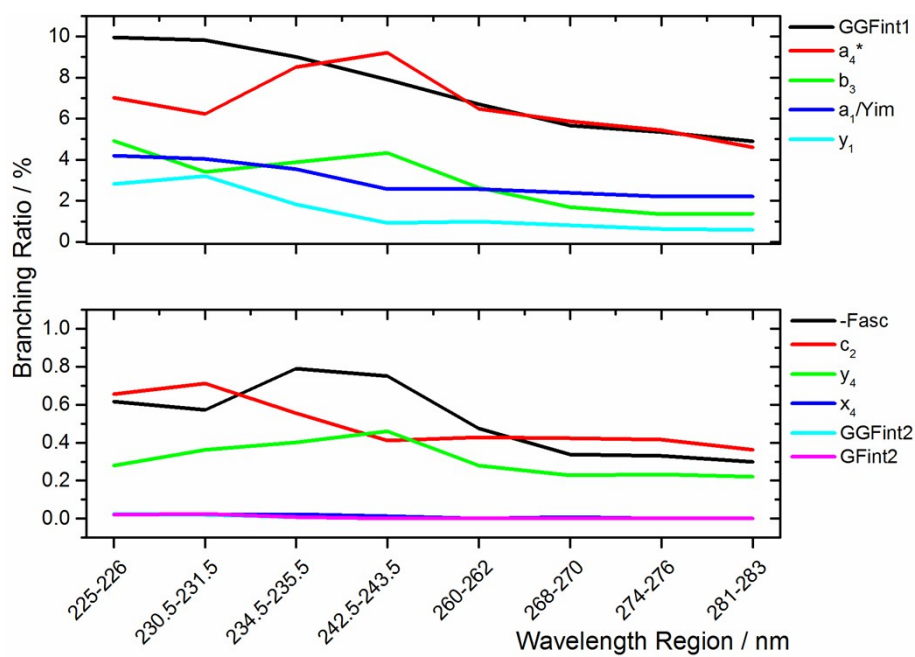
Very high abundance at short wavelengths (13):

YGGF int1, iu2, -Yasc-H, -H, Fasc, Yasc, YGGFL int1, GGF int4+H, YGGF int3+H, a₃, x₃, c₁, b₁



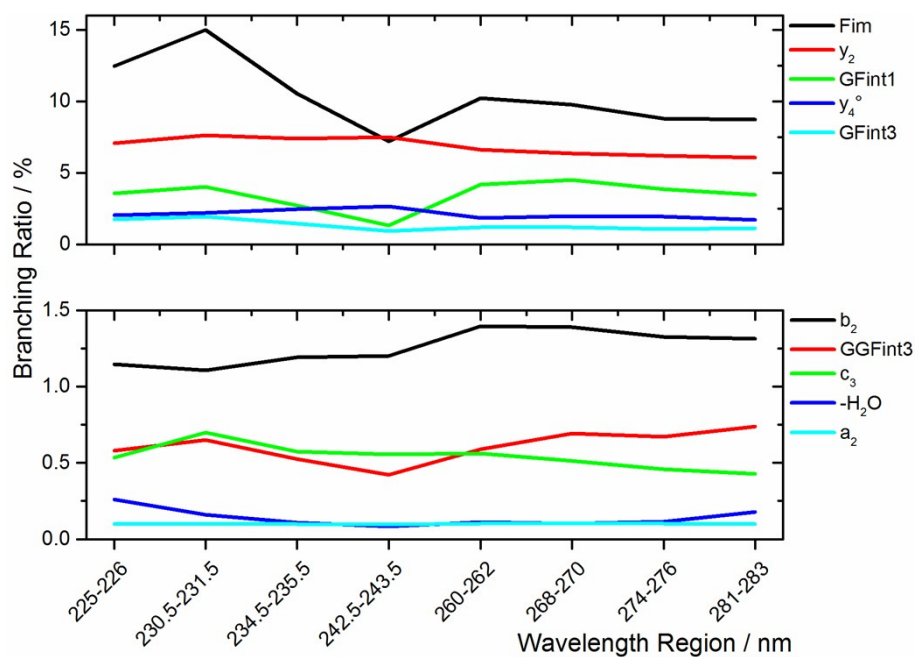
High abundance at short wavelengths (11):

GGF int1, a₄^{*}, b₃, a₁/Yim, y₁, -Fasc, c₂, y₄, x₄, GGF int2, GF int2



Rather constant abundance at all wavelengths (10):

F im, y_2 , GF int1, y_4° , GF int3, b_2 , GGF int3, c_3 , $-H_2O$, a_2



High abundance at long wavelengths (8):

a_4 , iu1, b_4 , -Yasc, y_3 , $-(NH_3+HCOOH)$, YGGF int2, -HCOOH

